ALEPH 98–063
CONF 98–033
8 July 1998

Abstract Registration Number 937
Parallel session: 9
Plenary session: 11

P R E L I M I N A R Y

Leptonic decays of the D_s meson

The ALEPH Collaboration

Abstract

The purely leptonic decays $D_s \to \mu\nu$ and $D_s \to \tau\nu$ are studied in a sample of four million hadronic Z decays collected in 1991–1995 with the ALEPH detector at LEP. A linear discriminant analysis is used to measure the branching fraction $B(D_s \to \mu\nu) = [0.64 \pm 0.08(\text{stat}) \pm 0.21(\text{syst}) \pm 0.15(\text{BR})]\%$. Within the Standard Model, this result corresponds to $f_{D_s} = [284 \pm 18(\text{stat}) \pm 49(\text{syst}) \pm 34(\text{BR})]$ MeV.

ALEPH contribution to 1998 summer conferences
Contact person: John Putz (John.Putz@cern.ch)

1 Introduction

The branching fraction of the D_s to a lepton and a neutrino is interesting because in the quark model it represents the annihilation of the D_s meson's constituent quark and anti-quark. The rate of these decays is governed partly by the quark–anti-quark wavefunction at the origin. This quantity is parametrized by the D_s decay constant f_{D_s}. Besides its own intrinsic interest this measurement is useful because it sheds light on the theoretical understanding of the decay constants of other heavy mesons. The B and B_s meson decay constants influence the B-$\bar{B}$ mixing rates. At present these decay constants cannot be measured experimentally, so the interpretation of mixing measurements depends on theoretical calculations. Better experimental determination of f_{D_s} will serve as a valuable check on these calculational techniques. Knowing the values of f_B and f_{B_s} will allow for the extraction of the third generation CKM matrix elements from the B mixing measurements and further constrain the three-generation mixing unitarity triangle.

The branching fraction for the leptonic decay $D_s \to \ell\nu$ is given by

$$B(D_s \to \ell\nu) = \tau_{D_s} \frac{G_{\mathrm{F}}^2}{8\pi} f_{D_s}^2 |V_{cs}|^2 M_{D_s} M_\ell^2 \left(1 - \frac{M_\ell^2}{M_{D_s}^2}\right)^2 , \quad (1)$$

where τ_{D_s} is the lifetime of the D_s meson, G_{F} is the Fermi coupling constant, V_{cs} is a CKM matrix element, and M_ℓ and M_{D_s} are the lepton and D_s masses.

2 Data sample and event selection

The selection is optimized to select $e^+e^- \to c\bar{c}$ events containing the decay $D_s \to \mu\nu$. The preselection of hadronic Z decays is performed according to the standard ALEPH selection based on charged tracks. The cut on the minimum number of reconstructed charged tracks coming from the area of the interaction point is tightened to reduce the background from $e^+e^- \to \tau^+\tau^-$ events. The event thrust axis is required to satisfy $|\cos\theta_{\mathrm{thrust}}| < 0.8$ to select events within the acceptance of the vertex detector. A loose muon identification algorithm based on muon chamber hits and the digital pattern information from the hadron calorimeter is used to select muon candidates.

A kinematic fit is then performed in order to improve the resolution on the missing momentum, assumed to arise from the undetected neutrino from $D_s \to \mu\nu$. In this fit, the missing mass is constrained to be zero and the D_s displacement direction (from the primary event vertex to some point on the muon track) is constrained to be parallel to the D_s momentum direction. The energies of the reconstructed charged and neutral particles are varied in the fit, while their directions are held constant. The event primary vertex and the D_s decay vertex are also allowed to vary within their uncertainties. The energy resolutions for charged, neutral electromagnetic, and neutral hadronic objects are parametrized from simulated events. The fitted energy of the D_s candidate (the muon and the neutrino) is required to be greater than 15 GeV.

To reduce background from $b\bar{b}$ events, selections are made based on a set of rapidity and impact parameter dependent hemisphere variables. An existing ALEPH lifetime tag [3] was modified to include a dependence on the rapidity of the charged tracks in the event. Events from $c\bar{c}$ are expected to have higher rapidity tracks relative to the jet axes than $b\bar{b}$ events because of the lower mass of c hadrons compared to b hadrons. Additionally, if one excludes the identified muon, signal events will only have fragmentation tracks in the muon hemisphere, and can be distinguished from other $c\bar{c}$ events. The tracks in each hemisphere are divided according to whether their rapidity is greater or less than a certain value. The probabilities that the sets of high and low rapidity tracks in each hemisphere originate from the Z production point are then calculated. Cuts are made on the probabilites for the low rapidity tracks in each hemisphere, and on the high rapidity tracks' probability in the muon hemisphere.

Finally, to distinguish signal from the remaining primarily $c\bar{c}$ and $b\bar{b}$ background events a hard cut is made on the energy of the fitted D_s candidate ($> 25\,\text{GeV}$). The leptonic branching fractions are extracted by means of a fitting procedure which is designed to distinguish between the two principal background components separately. Two linear discriminant variables are created. One is constructed specifically to separate $c\bar{c} \to D_s \to \mu\nu$ events from $b\bar{b}$ background events (mainly containing semileptonic b and c decays), and another to separate them from $c\bar{c}$ background events (mainly containing semileptonic c decays). The linear discriminant variables U_b and U_c are linear combinations of variables which optimally distinguish between two distributions. Each linear discriminant variable is a linear combination of fifteen variables. Plots of the distributions for the $c\bar{c} \to D_s \to \mu\nu$ events and the respective background events are shown in Fig. 1.

The procedure to fit for the $D_s \to \mu\nu$ (plus $D_s \to \tau\nu$) component in the data consists of fitting slices of the invariant mass distribution of the μ and ν combination in 36 bins (6×6) in the (U_b, U_c) plane simultaneously. Fitting functions are generated by separately fitting the mass distributions for each event type in each slice. One to three Gaussians are used depending on the number of events in the slice. The fits for each event type are normalized to one another according to the Monte Carlo predictions. In the fit to the data the backgrounds are divided into two categories, $b\bar{b}$ events and all other events (including $udsc$ events and the few remaining $e^+e^- \to \tau^+\tau^-$ events). The normalization of each background component is allowed to vary separately, while the shapes are fixed. The signal distribution combines the purely leptonic D_s decays from $c\bar{c}$ and $b\bar{b}$ events; it includes a small fraction from $D^+ \to \mu\nu$ and $D^+ \to \tau\nu$ which are nearly indistinguishable from D_s leptonic decays. The constraint $B(D_s \to \tau\nu)/B(D_s \to \mu\nu) = 9.75$ (from Eq. 1) is imposed.

3 Results

The fit to the data, summed over all 36 slices, is shown in Fig. 2. Figure 3 shows the data plus the fitted composition of Monte Carlo events for each of four regions in the (U_b, U_c) plane.

The fitted branching fraction is $B(D_s \to \mu\nu) = (0.670 \pm 0.083)\%$. The fitted number of signal events is 747 ± 93, while the total number of background events is 5496. The individual contributions are shown in Table 1.

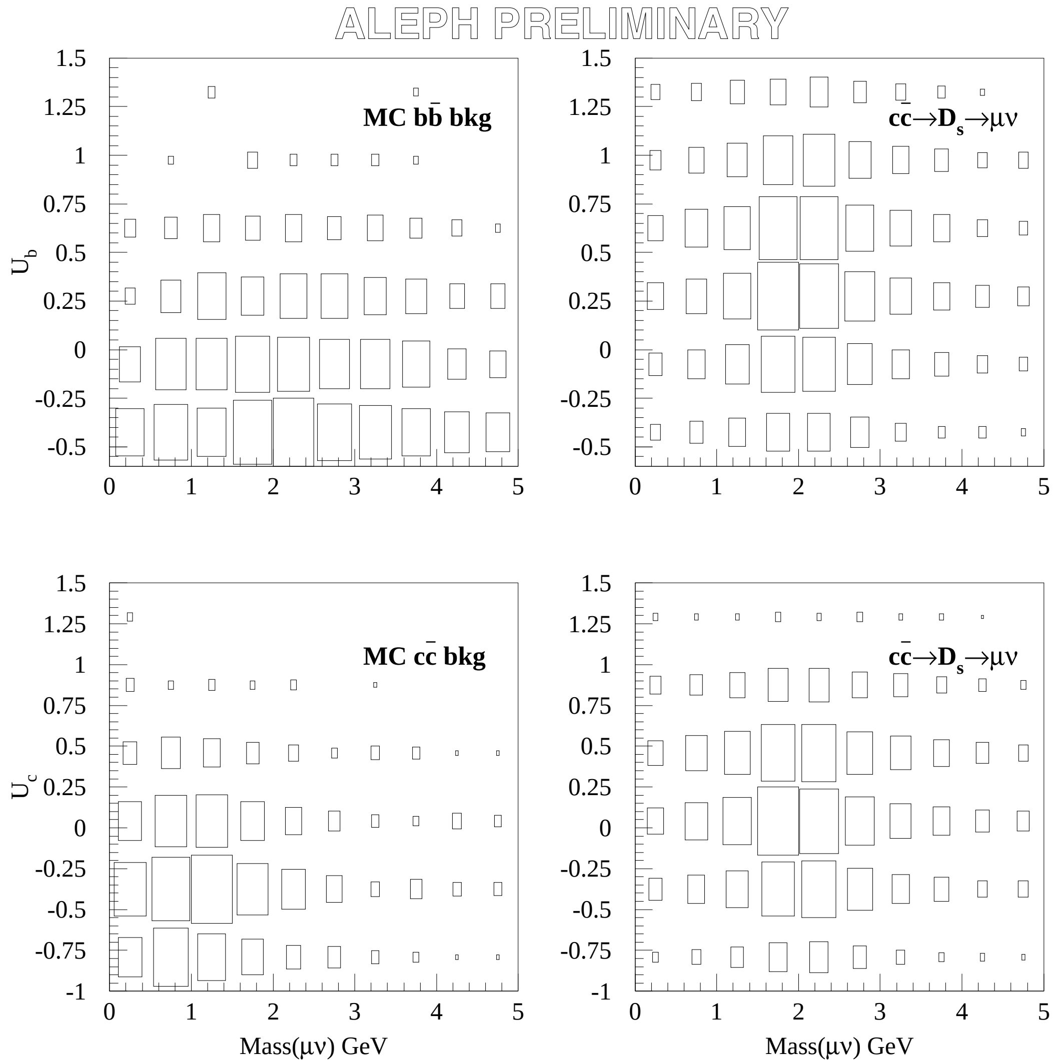

Figure 1: Unnormalized U_b vs $M(\mu\nu)$ (top) and U_c vs $M(\mu\nu)$ (bottom) distributions for $b\bar{b}$ background (left) and $c\bar{c} \rightarrow D_s \rightarrow \mu\nu$ (right), and $c\bar{c}$ background and $c\bar{c} \rightarrow D_s \rightarrow \mu\nu$, respectively. The same cuts used in the fitting procedure are applied here.

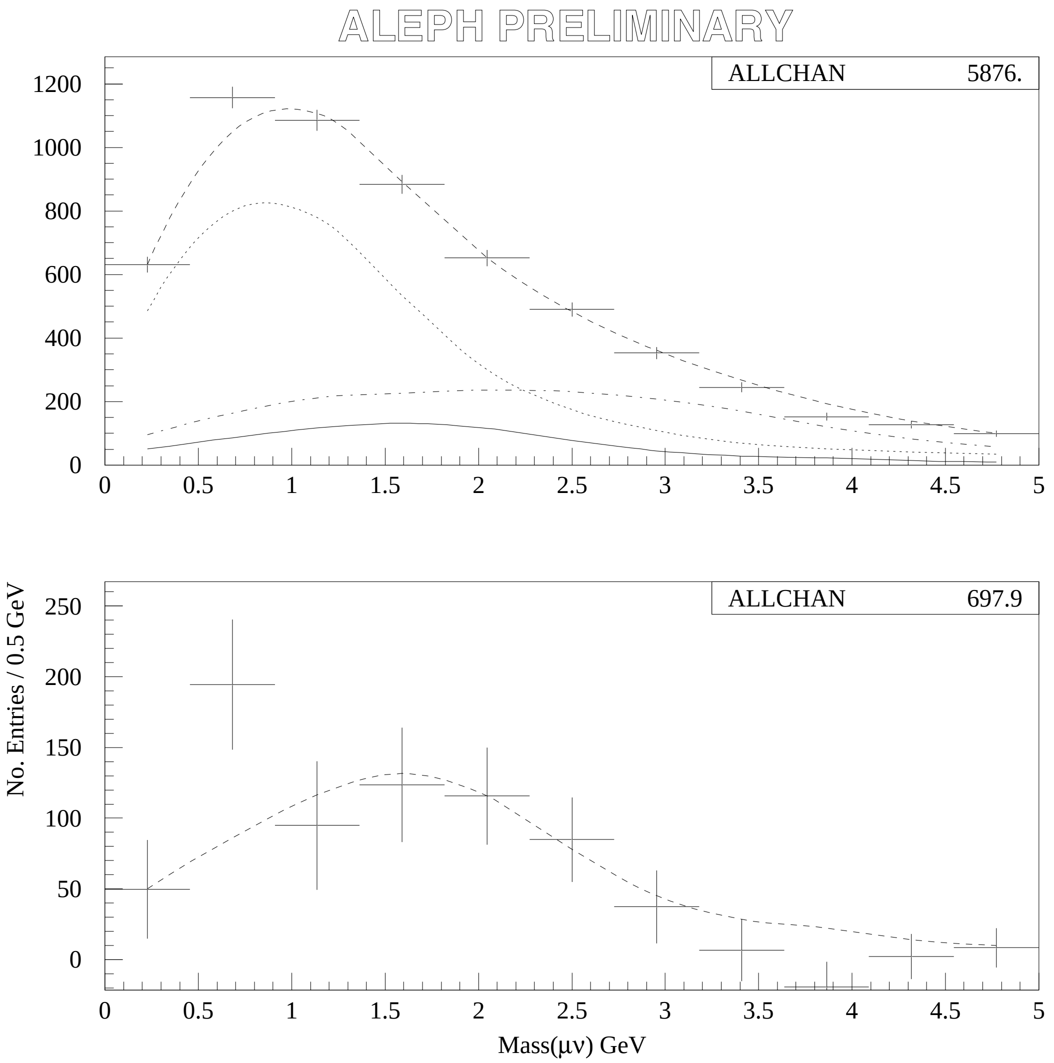

Figure 2: The fit to the mass distribution in the data summed over all 36 slices. The data are the crosses. The top plot shows the data and the fitted contributions. The dashed curve is the sum of all contributions. The dot-dash curve shows the $b\bar{b}$ background events. The dotted curve is the *udsc* background. The solid curve is the signal. The bottom plot shows the data minus the background, and the curve is the fitted signal contribution.

Table 1: Fitted numbers of events in the individual signal and background components.

Source	No. Events
Signal:	
$c\bar{c} \to D_s \to \mu\nu$	185
$c\bar{c} \to D_s \to \tau\nu$	386
$b\bar{b} \to D_s \to \mu\nu$	108
$b\bar{b} \to D_s \to \tau\nu$	23
$D^+ \to \ell\nu$	46
Total	747
Background:	
uds	593
$c\bar{c}$	2864
$b\bar{b}$	2024
$\tau^+\tau^-$	15
Total	5496

4 Systematic uncertainties

There is a small bias in the fitting procedure when run on Monte Carlo events. The fitted signal amplitude is overestimated by a factor of 1.048. The fractional uncertainty due to the limited Monte Carlo statistics is 0.087.

The production fractions of charmed mesons in $b\bar{b}$ and $c\bar{c}$ events are renormalized according to the most recent ALEPH measurements. Applying the corrections to the Monte Carlo distributions produces a shift in the fitted leptonic branching fraction. The production fractions are also varied according to their experimental uncertainties. The sum in quadrature of the variations in the resulting branching fraction measurement plus half the shift is taken as the uncertainty on the branching fraction measurement.

The uncertainty in the signal efficiency due to the muon identification efficiency and the uncertainty on the fragmentation parameter for the signal events is estimated. The muon efficiency is reduced by 20% in the Monte Carlo for muons with $P < 3\,\mathrm{GeV}$ and the data is refitted. The uncertainty due to fragmentation is estimated by lowering the energy cut on the D_s candidate by 2%. The resulting change in the fraction of signal events predicted by Monte Carlo is taken as the uncertainty.

A check on the assumed $\tau\nu/\mu\nu$ signal ratio is done by allowing the $\tau\nu$ and $\mu\nu$ branching fractions to vary independently. The results of this fit are $B(D_s \to \mu\nu) = (0.596 \pm 0.246)\%$ and $B(D_s \to \tau\nu)/B(D_s \to \mu\nu) = 11.8 \pm 7.0$, consistent with the branching fraction fitted above and with the expected $\tau\nu/\mu\nu$ ratio of 9.75.

There remain other significant systematic errors to estimate. The fragmentation parametrization needs to be varied. The composition and properties of the principal background components need to be understood. A check on the fit can also be performed by running the analysis to look for $D_s \to e\nu$, which is expected to be extremely small due to helicity suppression. The signal efficiency can be better estimated by analyzing $D_s \to \phi\pi$ decays. The reason for the bias in the fitting routine needs to be understood.

Table 2: Summary of systematic errors.

Source	Fractional uncertainty
Fit bias $\pm$ MC statistics	$+0.048 \pm 0.087$
Hadron production fractions:	
$\Delta/2$	0.032
σ	± 0.056
Physics parameters:	
$f(c \to D_s)$	$\pm 0.133 \pm 0.195$ (BR)
$f(c \to D^+)$	± 0.005
$f(b \to D_s)$	$\pm 0.019 \pm 0.041$ (BR)
$f(b \to D^+)$	± 0.001
$B(D^+ \to \mu\nu)/B(D_s \to \mu\nu)$	± 0.003
$B(D^+ \to \tau\nu)/B(D_s \to \mu\nu)$	± 0.002
Signal efficiency:	
μ identification	± 0.01
Fragmentation	± 0.04
Background shape:	
($\sim 5\times$ hadron prod unc)	± 0.30
Total bias and uncertainty	$+0.05 \pm 0.34 \pm 0.24$ (BR)

The effect of detector resolution on the results must be examined.

Table 2 summarizes the systematic uncertainties which have been estimated. The uncertainties under the heading physics parameters refer to uncertainties on the signal. The largest component comes from $f(c \to D_s)$ which almost corresponds to the overall normalization of the signal, since the contributions from the $b\bar{b} \to D_s \to \mu\nu$ and $D^+ \to \ell\nu$ channels are small. The errors labelled (BR) refer to the uncertainty in the measurement of $D_s \to \phi\pi$. The background shape uncertainty is a conservative estimate which includes as yet unaccounted for effects relating to the shape of the background distributions.

5 Conclusions

A preliminary measurement of $B(D_s \to \mu\nu)$ has been made. The result is $B(D_s \to \mu\nu) = [0.64 \pm 0.08 \pm 0.21 \pm 0.15(\text{BR})]\%$. This value corresponds to $B(D_s \to \tau\nu) = 6.2\%$, under the assumption $B(D_s \to \tau\nu)/B(D_s \to \mu\nu) = 9.75$ which is assumed in the fit to the data. The decay constant f_{D_s} is calculated to be $[284 \pm 18 \pm 49 \pm 34(\text{BR})]$ MeV.

References

[1] L3 Collaboration, Phys. Lett. B 396 (1997) 327.

[2] DELPHI Collaboration, International Europhysics Conference on High Energy Physics, Jerusalem, 19–26 August 1997, contributed paper 455.

[3] ALEPH Collaboration, D. Buskulic *et al.*, Phys. Lett. **B313** (1993) 535.

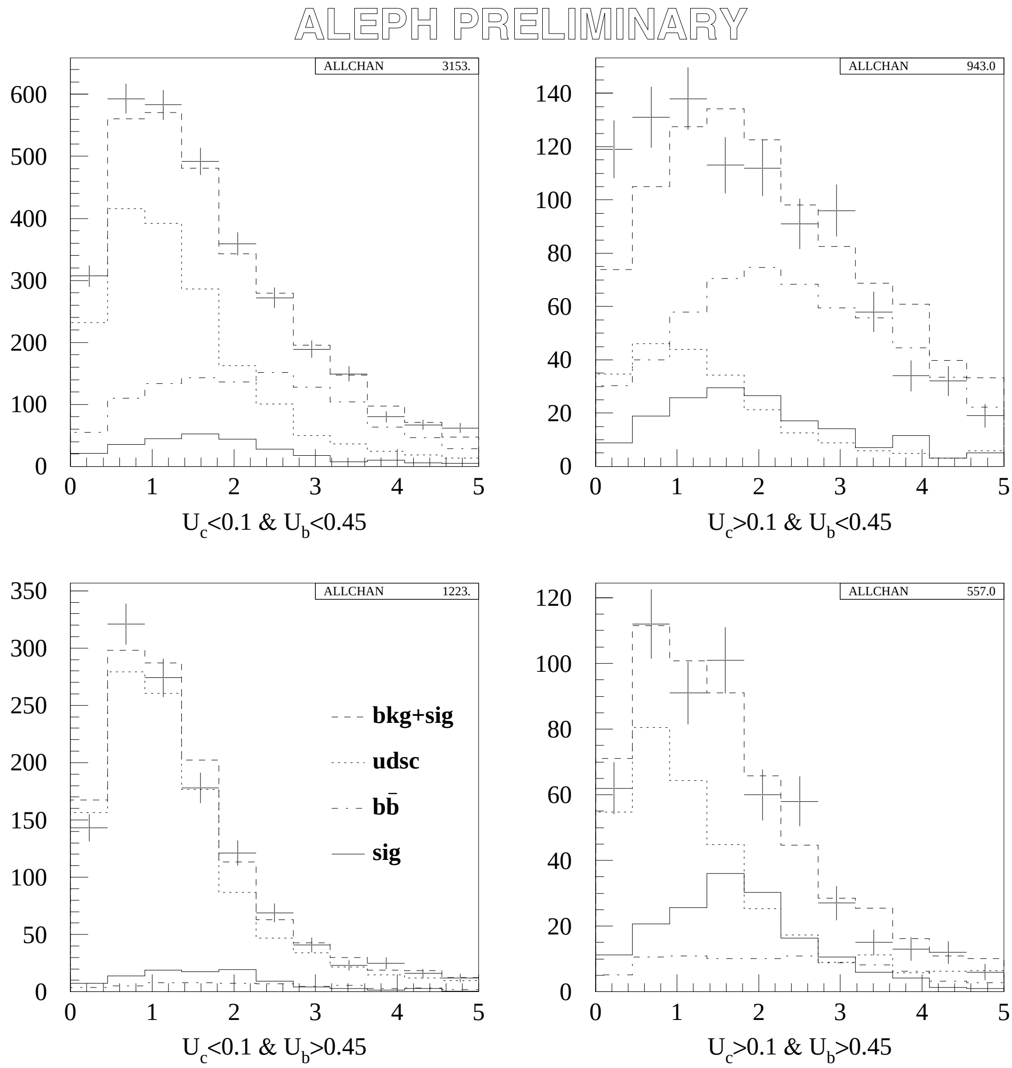

Figure 3: Data divided into four regions in the (U_b, U_c) plane. The histograms are the fitted contributions from *udsc* background, $b\bar{b}$ background, and signal events.